Supplemental Data

The *C. elegans* Zonula Occludens Ortholog Cooperates with the Cadherin Complex to Recruit Actin during Morphogenesis

Christina Lockwood, Ronen Zaidel-Bar, and Jeff Hardin

Supplemental Results

Characterization of zoo-1 alleles

To examine consequences of loss of *zoo-1* function, we analyzed two *zoo-1* mutants, *gk404*, a 946-bp deletion of the first exon and surrounding promoter sequence, and *cxTi8317*, which contains a Tc5 transposon insertion predicted to disrupt the resulting GuK and Zu5 domains of ZOO-1 (Supplemental Figure 1). Neither allele confers a readily discernable phenotype; immunostaining reveals that ZOO-1 protein is produced in both backgrounds (data not shown). Although *zoo-1(gk404)* deletes exon 1 and the surrounding bases, we found that a message is indeed produced in *gk404* homozygotes that initiates from Met3 at the start of the second exon (data not shown). These data indicate that *gk404* and *cxTi8317* provide incomplete loss of *zoo-1* gene function.

Supplemental Experimental Procedures

C. elegans alleles and strains

Bristol N2 was used as the wild-type strain [1]. Nematodes were grown at 20°C in all experiments and were cultured as described [1]. *zoo-1(cxTi8317)* was kindly provided by L. Segalat [2]. All other strains were either constructed in our laboratory or obtained from the *Caenorhabditis* Genetics Center. The following mutations were used. LGI: *zoo-1(cxTi8317* and

gk404), hmp-2 (qm39) [3]. LGII: *rrf-3(pk1426)* [4], *vab-9(ju6)* [5]; *mel-11(it26)* [6]. LGV: *hmp-1(zu278* and *fe4)* [7, 8], *sma-1(e30)* [9], *daf-11(m84)* [9]. LGX: *dlg-1(ok318)*. Strain SU295 contains an integrated array (*jcIs24*) that includes *jac-1::gfp* and has not been mapped to a LG [8]. Strain SU292 contains an integrated *zoo-1::gfp* array (*jcIs22*) that has not been mapped to a LG.

Sequence analysis and identification of lesions in zoo-1 alleles

Protein sequence comparisons were performed using online tools available at the European Bioinformatics Institute (http://www.ebi.ac.uk/Tools/emboss/align/) and domain structure was analyzed using online tools available at Simple Modular Architecture Research Tool (SMART) (http://smart.embl-heidelberg.de/). We obtained the *zoo-1(gk404)* allele from the *C. elegans* Knockout Consortium and performed six outcrosses. We identified the lesion by isolating genomic DNA from homozygous hermaphrodites and amplified the genomic region with primers TT110 and TT111. The resulting amplification products were sequenced and confirmed that *gk404* contains a 946 bp deletion that removes all of exon 1 (96 bp) and 850 bp of the surrounding bases.

zoo-1(cxTi8317) was obtained from L. Segalat and was outcrossed six times and the insertion was molecularly tracked since animals homozygous for *cxTi8317* do not have an observable phenotype. Single hermaphrodites were allowed to lay progeny for 24 hours before their genomic DNA was isolated for analysis. The primer pair TT27 and TT74 flanks the insertion site and does not produce a product if the transposon is present and a 1.6 Kb product in wild-type worms. Primer set TT33 and Tc5.04 was also used for confirmation and amplified a 500 bp product only if the Tc5 transposon was present.

Construction of zoo-1::gfp transgene and transformation

A translational ZOO-1::GFP expression construct was created by ligating 5 Kb of genomic *zoo-1* sequence upstream of exon 2 to a 3.1 Kb *PstI* restriction fragment of *zoo-1* cDNA from yk621c6 (Y. Kohara). A second construct contained the *dlg-1* promoter [10] ligated to the *zoo-1* coding region. The fused products were cloned into the GFP vector, pPD95.75 (A. Fire). Standard microinjection techniques were used to create worms carrying the extrachromosomal array *jcEx81* [*zoo-1::gfp*, pRF4] and *jcEx70* [*Pdlg-1::zoo-1*, pRF4]. *jcIs22* was created by integrating *jcEx81* by gamma irradiation as described [5].

RT-PCR

RT-PCR was performed using Superscript III reagents (Invitrogen, Carlsbad, CA) as described [11]. Briefly, cDNA was synthesized from wild type and *zoo-1(gk404)* hermaphrodites using an oligo-d(T) primer for first-strand synthesis. Amplification of *zoo-1* or *act-1* (a positive control) cDNA was performed with gene-specific primers. Since EST data suggests that *zoo-1* can be alternatively spliced to remove exon 9, primer sets were designed that are capable of recognizing transcripts from either isoform.

RNAi

Two RNAi delivery methods were used to knockdown *zoo-1* maternal and zygotic product: injection and feeding. For injection, *zoo-1* cDNA was subcloned into two fragments encompassing the entire cDNA to facilitate efficient RNA transcription. Primer set TT26 and TT13 amplified a 1.6 Kb product that corresponds to the 5' region of *zoo-1*. We also amplified the 3' *zoo-1* cDNA region with primer sets TT27 and TT28, though subsequent experiments indicated that the 5' subclone alone is sufficient for ZOO-1 depletion (data not shown). RNA was transcribed *in vitro* according to the manufacturer's instructions (MegaScript T3 and T7 kits,

Ambion, Austin, TX). An ethanol ammonium acetate precipitation was used to recover RNA and product concentration was assessed by OD260 and confirmed by gel electrophoresis. Single-stranded RNA was diluted to an injection concentration of 2 μg/μl and sense/antisense annealing was carried out through incubation at 70°C for 10 minutes followed by incubation at 37°C for 30 minutes.

To construct a feeding clone, the 1.6 Kb *zoo-1* cDNA region that was successful for injection RNAi was subcloned into pPD129.36 using the *XbaI* and *HindIII* restriction sites and the resulting plasmid was transformed into HT115(DE3) bacteria. RNAi by feeding was performed essentially as described [12, 13].

cDNA clones obtained from Y. Kohara (Gene Network Lab, NIG, Japan) included: yk621c6 (*zoo-1*), yk36d4 (*hmp-1*), yk1047c6 (*hmp-2*), yk1230g8 (*hmr-1*), yk25e5 (*dlg-1*), yk304e5 (*clc-1*). RNA template for *clc-2* was produced by PCR amplification of genomic DNA using nested primers with the T3 or T7 promoter sequence added.

Permeability and contractility sensitivity assays

A dye tracer experiment was performed essentially as described [14]. In all observed animals, the pharynx/intestine was outlined without body cavity leakage. To test for sensitivity of *zoo-1(RNAi);rrf-3* embryos to changes in actomyosin contractility, we performed two experiments. To reduce *let-502* function, we performed feeding RNAi using *rrf-3* worms fed bacteria expressing either *zoo-1* and *let-502* dsRNA, or *zoo-1* dsRNA and an equivalent amount of L4440 bacteria. After 24 hr of feeding, worms were cut open, the embryos were extracted, and allowed to develop overnight on a watch glass. Embryos arrested during elongation were then counted. To examine effects of reducing *mel-11* activity, we performed *zoo-1* feeding RNAi on *mel-11(it26)* mutants, and

compared the results to *mel-11(it26)* alone. Embryos rupturing prior to 1.5-fold, after 1.5-fold, or exhibiting no rupture were scored from 4D movies. Statistical analyses were performed online using Fisher's 2 x 2 exact test or 2 x 3 test (http://www.quantitativeskills.com/sisa/statistics/fiveby2.htm).

Antibodies and embryo staining

For immunostaining, embryos were freeze cracked as described [7] and stained as described [5]. Embryos were fixed and prepared for staining with the following antibodies diluted in PBS with 1% BSA: affinity purified rabbit-α-ZOO-1 (Proteintech Group Inc., Chicago, IL; 1:500), monoclonal antibody (mAb) MH27 against AJM-1 ([15]; 1:50), mAb2085 against HMP-1 (Chemicon, Temecula, CA; 1:50). Double labeling with phalloidin and antibody was performed as described [8, 16].

Microscopy

4D Nomarski microscopy was performed as previously described [17]. Embryos were filmed on a Nikon Eclipse E600 or Optiphot-2 upright microscope equipped with DIC optics. NIH Image and ImageJ software were used to compress data into 4D QuickTime movies with custom macros/plugins (available at http://worms.zoology.wic.edu/4d/4d.html). Live imaging of GFP-expressing embryos was performed via spinning disc confocal microscopy with a Yokogawa CSU10 scanhead and a Hamamatsu ORCA-ER CCD camera. Fixed specimens were visualized using spinning disc confocal microscopy and collected with Perkin Elmer Ultraview software. In some figures, multiple focal planes were projected to generate images. For quantification of F-actin intensity, images were imported into and analyzed using the public domain program Priism [18], available at http://msg.ucsf.edu/IVE/index.html. For colocalization analysis, junctions from embryos immunostained for ZOO-1 and AJM-1, or stained for ZOO-1

and expressing JAC-1::GFP were 3d projected using ImageJ software. The resulting reconstructed junctional boundaries were manually traced and the relevant ROI was subjected to colocalization analysis using a plugin for ImageJ written by T. Collins, McMaster University (available at http://www.macbiophotonics.ca/imagej/installing_imagej.htm). Statistical analyses were performed using Microsoft Excel.

Supplemental References

1. Brenner, S. (1974). The genetics of Caenorhabditis elegans. Genetics *77*, 71-94.
2. Martin, E., Laloux, H., Couette, G., Alvarez, T., Bessou, C., Hauser, O., Sookhareea, S., Labouesse, M., and Segalat, L. (2002). Identification of 1088 new transposon insertions of Caenorhabditis elegans: a pilot study toward large-scale screens. Genetics *162*, 521-524.
3. Hekimi, S., Boutis, P., and Lakowski, B. (1995). Viable maternal-effect mutations that affect the development of the nematode Caenorhabditis elegans. Genetics *141*, 1351-1364.
4. Simmer, F., Tijsterman, M., Parrish, S., Koushika, S.P., Nonet, M.L., Fire, A., Ahringer, J., and Plasterk, R.H. (2002). Loss of the putative RNA-directed RNA polymerase RRF-3 makes C. elegans hypersensitive to RNAi. Curr Biol *12*, 1317-1319.
5. Simske, J.S., Koppen, M., Sims, P., Hodgkin, J., Yonkof, A., and Hardin, J. (2003). The cell junction protein VAB-9 regulates adhesion and epidermal morphology in C. elegans. Nat Cell Biol *5*, 619-625.
6. Wissmann, A., Ingles, J., McGhee, J.D., and Mains, P.E. (1997). Caenorhabditis elegans LET-502 is related to Rho-binding kinases and human myotonic dystrophy kinase and interacts genetically with a homolog of the regulatory subunit of smooth muscle myosin phosphatase to affect cell shape. Genes Dev *11*, 409-422.
7. Costa, M., Raich, W., Agbunag, C., Leung, B., Hardin, J., and Priess, J.R. (1998). A putative catenin-cadherin system mediates morphogenesis of the Caenorhabditis elegans embryo. J Cell Biol *141*, 297-308.
8. Pettitt, J., Cox, E.A., Broadbent, I.D., Flett, A., and Hardin, J. (2003). The Caenorhabditis elegans p120 catenin homologue, JAC-1, modulates cadherin-catenin function during epidermal morphogenesis. J Cell Biol *162*, 15-22.
9. McKeown, C., Praitis, V., and Austin, J. (1998). sma-1 encodes a betaH-spectrin homolog required for Caenorhabditis elegans morphogenesis. Development *125*, 2087-2098.
10. Lockwood, C.A., Lynch, A.M., and Hardin, J. (2008). Dynamic analysis identifies novel roles for DLG-1 subdomains in AJM-1 recruitment and LET-413-dependent apical focusing. J Cell Sci *121*, 1477-1487.

11. Thomas-Virnig, C.L., Sims, P.A., Simske, J.S., and Hardin, J. (2004). The inositol 1,4,5-trisphosphate receptor regulates epidermal cell migration in Caenorhabditis elegans. Curr Biol *14*, 1882-1887.
12. Kamath, R.S., Fraser, A.G., Dong, Y., Poulin, G., Durbin, R., Gotta, M., Kanapin, A., Le Bot, N., Moreno, S., Sohrmann, M., et al. (2003). Systematic functional analysis of the Caenorhabditis elegans genome using RNAi. Nature *421*, 231-237.
13. Timmons, L. (2006). Delivery methods for RNA interference in C. elegans. Methods Mol Biol *351*, 119-125.
14. Asano, A., Asano, K., Sasaki, H., Furuse, M., and Tsukita, S. (2003). Claudins in Caenorhabditis elegans: their distribution and barrier function in the epithelium. Curr Biol *13*, 1042-1046.
15. Koppen, M., Simske, J.S., Sims, P.A., Firestein, B.L., Hall, D.H., Radice, A.D., Rongo, C., and Hardin, J.D. (2001). Cooperative regulation of AJM-1 controls junctional integrity in Caenorhabditis elegans epithelia. Nat Cell Biol *3*, 983-991.
16. Costa, M., Draper, B.W., and Priess, J.R. (1997). The role of actin filaments in patterning the Caenorhabditis elegans cuticle. Dev Biol *184*, 373-384.
17. Raich, W.B., Agbunag, C., and Hardin, J. (1999). Rapid epithelial-sheet sealing in the Caenorhabditis elegans embryo requires cadherin-dependent filopodial priming. Curr Biol *9*, 1139-1146.
18. Chen, H., Clyborne, W., Sedat, J.W., and Agard, D.A. (1992). PRIISM: an integrated system for display and analysis of three-dimensional microscope images. Proc. of SPIE *1660*, 784-790.

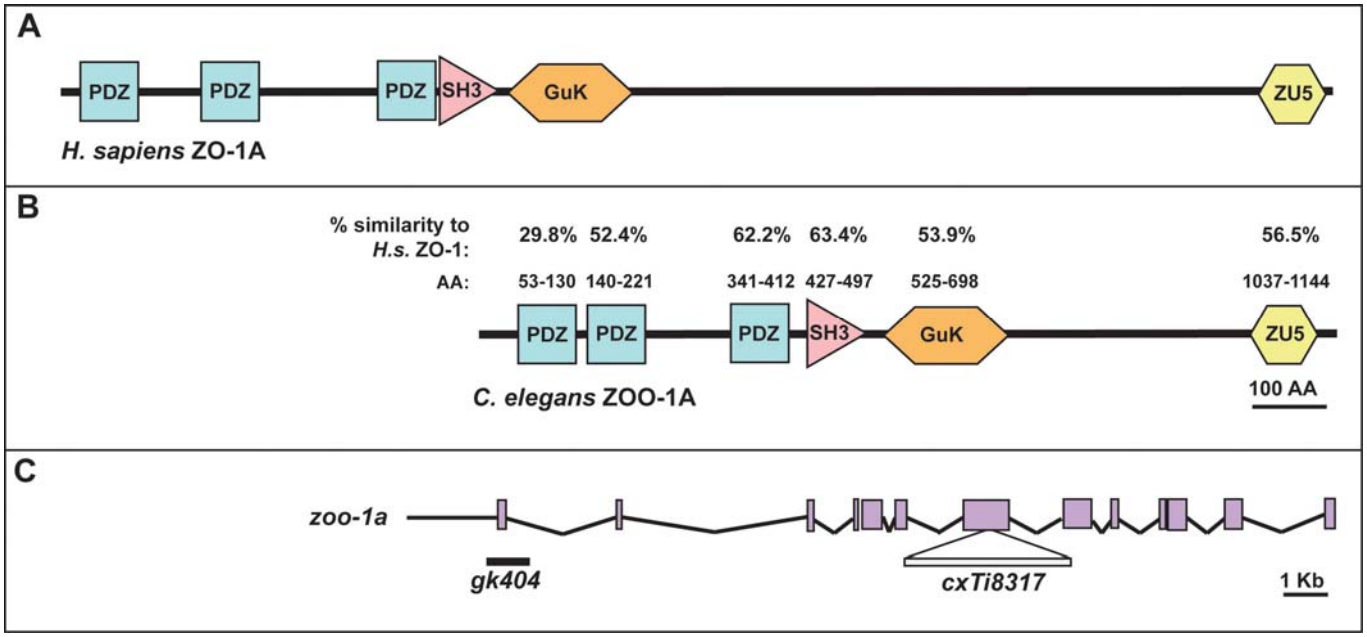

Figure S1. *zoo-1* encodes a *C. elegans* Zonula Occludens Ortholog.

Although the overall amino acid similarity of ZOO-1A to *Homo sapiens* ZO-1A is 34.2%, individual domains show much higher conservation. (A) Schematic structure of *H. sapiens* ZO-1A, which contains the following domains: PDZ, PSD-95, Dlg-1, ZO-1; SH3, Src Homology 3; GuK, Guanylate Kinase; ZU5, ZO-1, UNC-5 proline-rich region. (B) Schematic structure of ZOO-1. Amino acid residues of ZOO-1A corresponding to each region based on SMART predictions are indicated, as is the percent amino acid similarity within each domain compared to *H. sapiens* ZO-1A. (C) Structure of the *zoo-1* gene is shown with exons represented by boxes. Alleles *gk404* and *cxTi8317* are indicated.

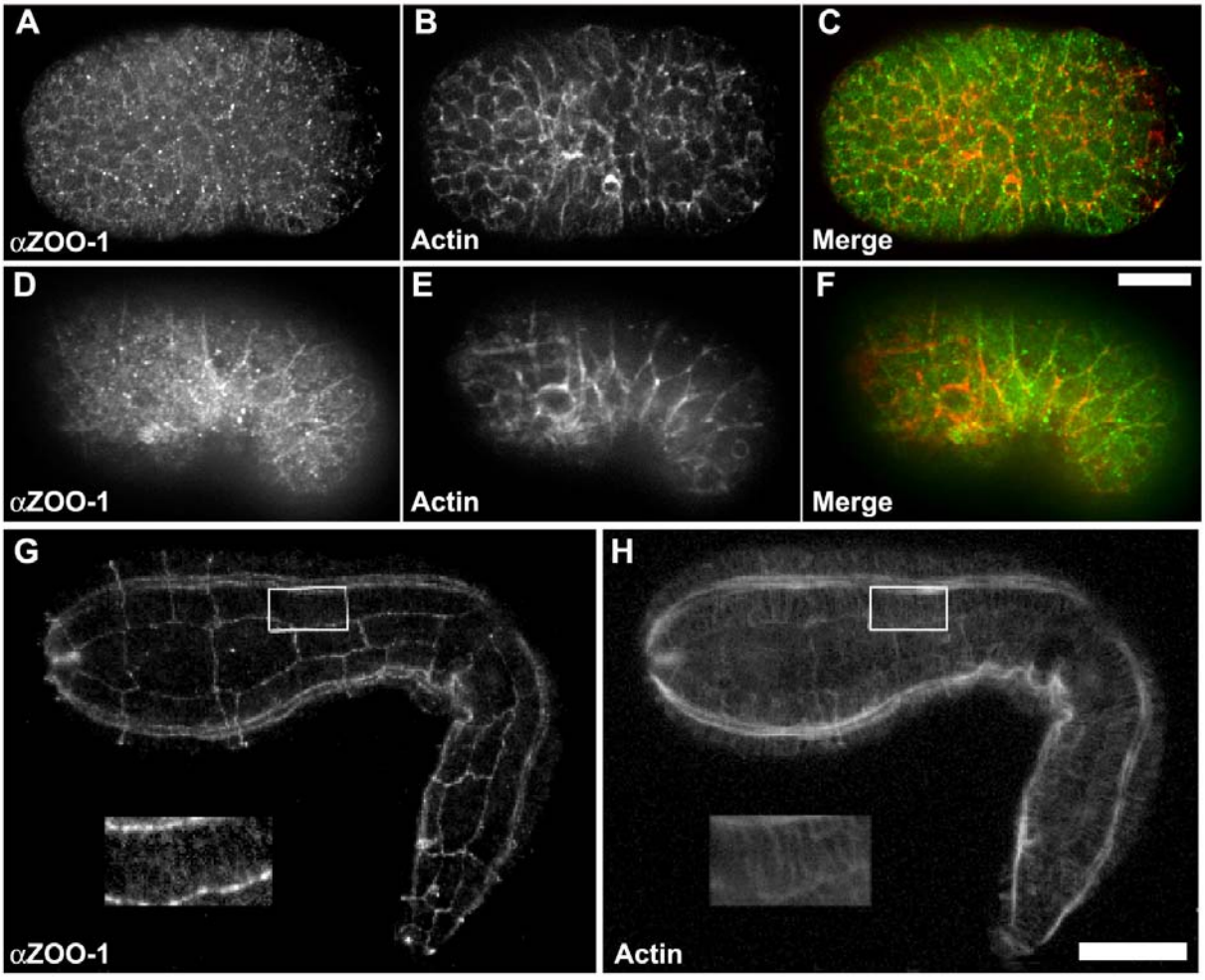

Figure S2. ZOO-1 colocalizes with actin at cell borders during morphogenesis.

Confocal images of embryos stained for ZOO-1 (A,D,G), F-actin (B,E,H), and the merge (C,F). (A-C) Embryo beginning ventral enclosure. (D-F) Embryo at the 1.25-stage of elongation has increased ZOO-1 at cell borders. (G, H) Embryo at the 2-fold stage of elongation has robust junctional ZOO-1. Insets in G and H are enlargements of the boxed regions. Scale bar, 10 μm.

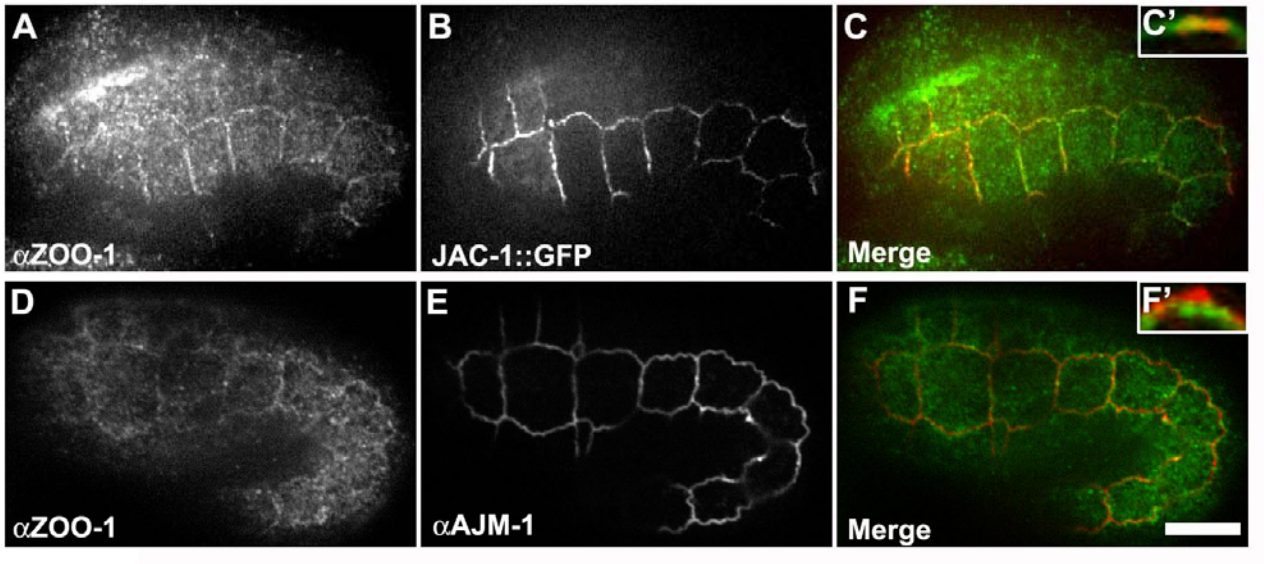

Figure S3. ZOO-1 colocalizes with the cadherin complex in the epidermis.

(A-C) Confocal images showing a comma stage embryo stained for ZOO-1 (A) that is also expressing JAC-1/p120-catenin::GFP (B). The merged image is shown in C (ZOO-1, red; JAC-1, green). C' shows a projected region of a junction in sagittal profile enlarged 3X. (D-F) Confocal images of a 1.5-fold stage embryo stained for ZOO-1 (D) and AJM-1 (E). The merged image is shown in F (ZOO-1, red; AJM-1, green). F' shows a projected region of a junction in sagittal profile enlarged 3X. Scale bar, 10 μm. Quantitative colocalization analysis confirms that ZOO-1 colocalizes with the cadherin complex. For JAC-1, $r^2 = 0.72 \pm 0.05$, mean ± SEM, n = 3, whereas for AJM-1, $r^2 = 0.39 \pm 0.05$, n = 3 (significantly different from JAC-1, $p < 0.004$, Fisher's exact test).

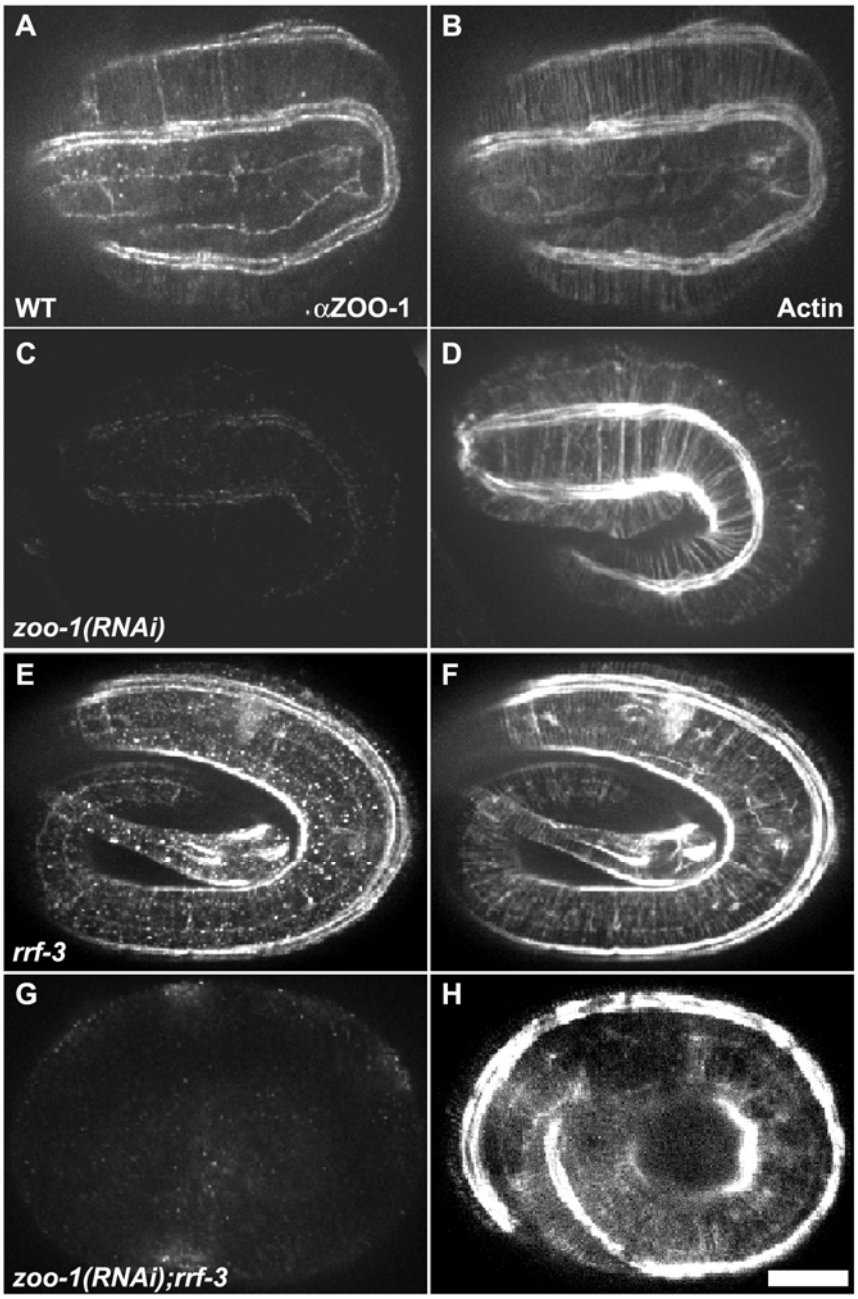

Figure S4. *zoo-1(RNAi);rrf-3(pk1426)* gene knockdown abolishes antibody signal. Embryos are stained for ZOO-1 (left column) and F-actin (right column). (A, B) Wild-type two-fold embryo corresponding to Figure 3E. (C, D) Two-fold *zoo-1(RNAi)* embryo, corresponding to Figure 3F. (E, F) Three-fold *rrf-3(pk1426)* embryo. (G, H) Three-fold *zoo-1(RNAi);rrf-*

3(pk1426) embryo. Compare residual levels of ZOO-1 in a *zoo-1(RNAi)* background (C) versus complete absence of ZOO-1 in *zoo-1(RNAi);rrf-3(pk1426)* (G). Scale bar, 10 μm.

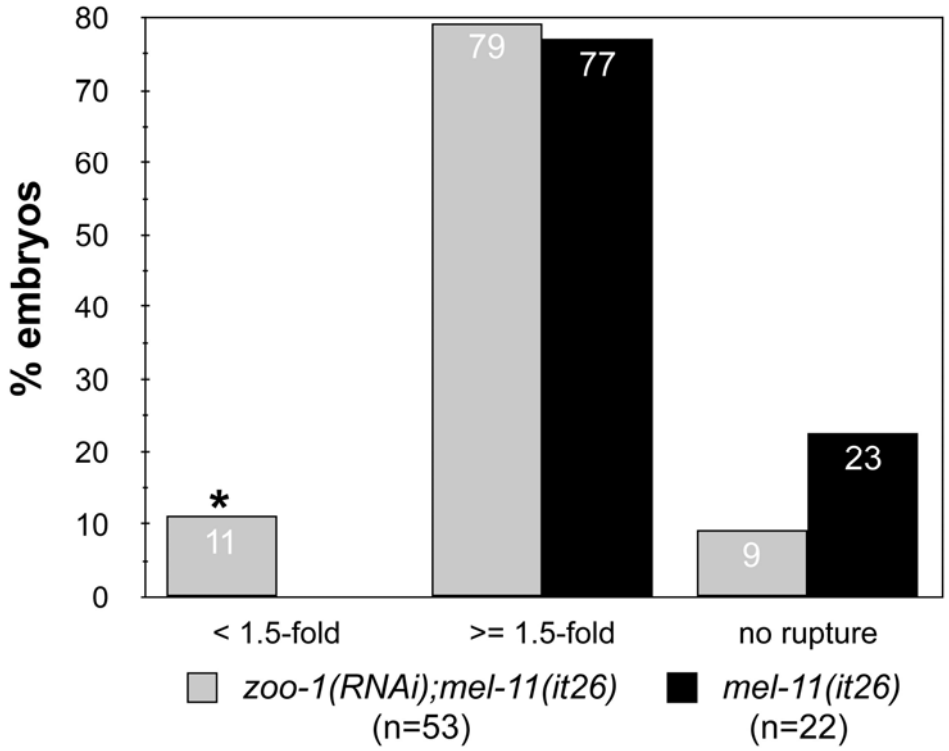

Figure S5. Loss of *zoo-1* function enhances rupture defects in *mel-11(it26)* hypercontractile mutants.

The percentage arrested at various stages of elongation was scored for *zoo-1(RNAi); mel-11(it26)* and *mel-11(it26)* embryos. Asterisk: significantly different, $p < 0.001$ (Fisher's exact test).

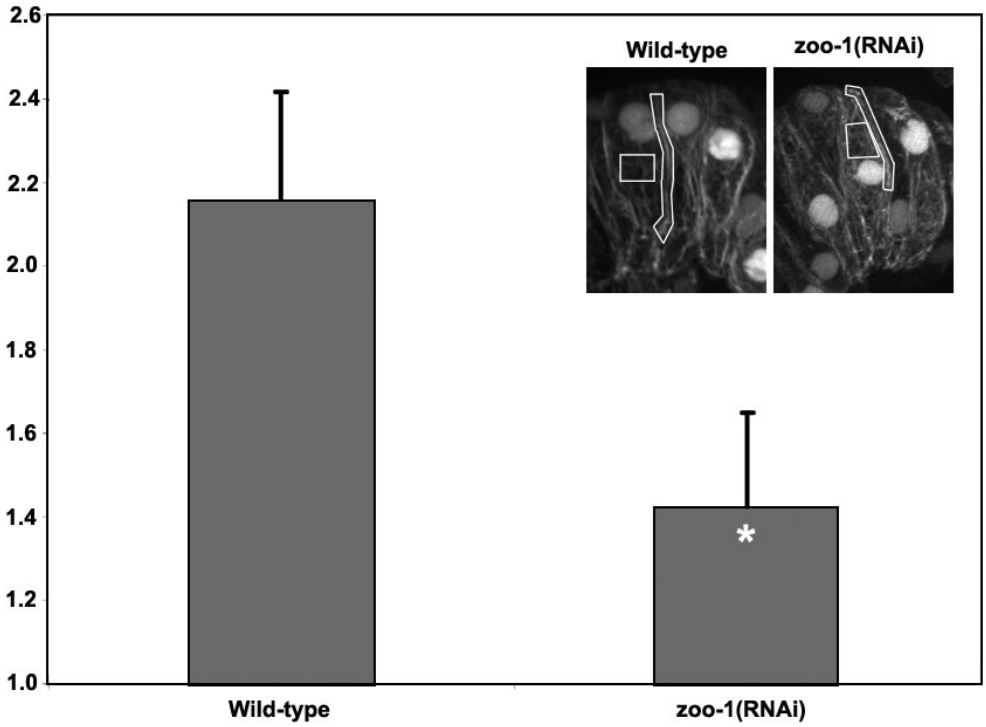

Figure S6. *zoo-1(RNAi);rrf-3* embryos accumulate less actin at cell borders.

The ratio of junctional to cytoplasmic actin was measured as described in Materials and Methods. Sample ROIs for representative wild-type and *zoo-1(RNAi);rrf-3* embryos are shown (inset). Asterisk: significantly different, $p < 0.01$(two-tailed student t-test).